

Very high frequency (~100 MHz) Plasma Enhanced Atomic Layer
Deposition High- κ Hafnium Zirconium Oxide Capacitors near
Morphotropic Phase Boundary with Low current density@0.8V of
 2×10^{-8} A/cm² & high- κ of 70 for DRAM Technology

Ketong Yang^a, Hunbeom Shin^a, Seungyeob Kim^a, Taeseung Jung^a, and Sanghun Jeon^{a,}*

a. School of electrical engineering, Korea Advanced Institute of Science and
Technology, 291 Daehak-ro, Yuseong-gu, Daejeon 34141, Korea

*Corresponding authors: E-mail: jeonsh@kaist.ac.kr

This file includes:

Figure S1. MPB phase formation in RF-deposited and VHF-deposited HZO films.

Figure S2. GIXRD of RF-deposited and VHF-deposited HZO films.

Figure S3. Basic characteristics of the 5 nm and 6 nm MPB HZO (1:3).

Figure S4. Dielectric constant of RF-deposited and VHF-deposited HZO films with voltage.

Figure S5. The steps involved in a single deposition.

Figure S6. 10 different VHF HZO 5 nm (1:1) samples K value.

Table S1. Dielectric Constant of RF-deposited and VHF-deposited HZO films.

Table S2. Trap states energy level of our sample and other reported hafnia films.

Table S3. Deposition rate of the HZO (1:1) films.

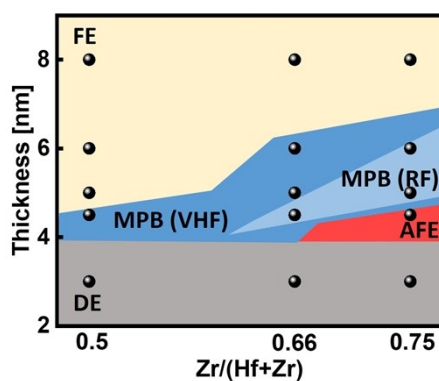


Figure S1. MPB phase formation in RF-deposited and VHF-deposited HZO films.

Figure S1 illustrates the formation of the MPB phase in HZO films treated with conventional RF and VHF methods. In VHF-processed HZO films, the MPB phase forms at lower Zr doping ratios and manifests across a wider range of thickness conditions compared to RF-processed films.

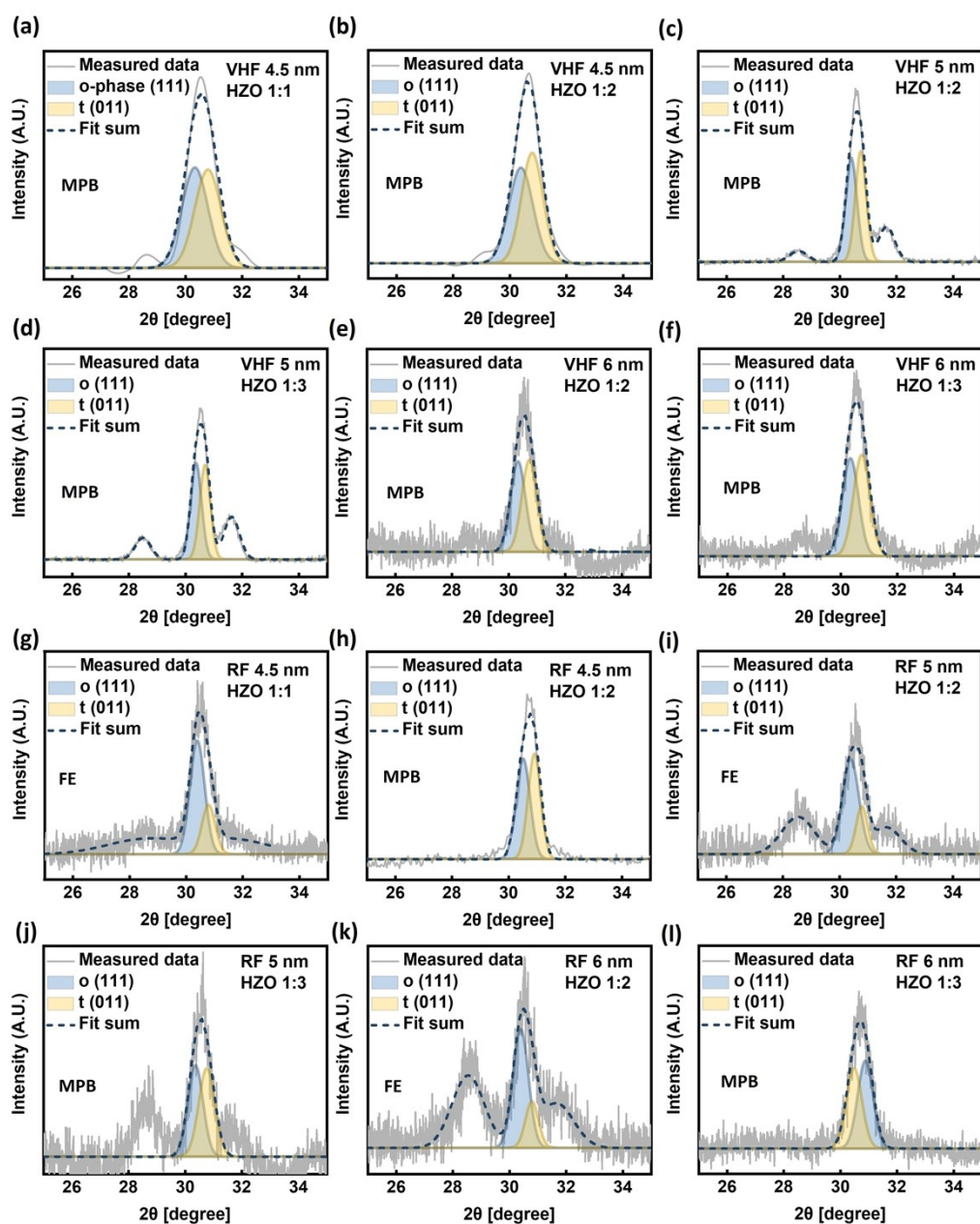


Figure S2. GIXRD of RF-deposited and VHF-deposited HZO films. VHF HZO shows MPB characteristics at 4.5 nm 1:1 (a), 4.5 nm 1:2 (b), 5 nm 1:2 (c), 5 nm 1:3 (d), 6 nm 1:2 (e), 6 nm 1:3 (f). RF HZO only shows MPB characteristics at 4.5 nm 1:2 (h), 5 nm 1:3 (j), 6 nm 1:3 (l). It shows ferroelectricity at 4.5 nm 1:1 (g), 5 nm 1:2 (i), 6 nm 1:2 (k).

The properties of HZO—ferroelectricity (FE), morphotropic phase boundary (MPB), and antiferroelectricity (AFE)—are primarily determined by the o-phase (111) and t-

phase (111), observed at 30.4° and 30.8° , respectively. When the o-phase is dominant, the sample exhibits ferroelectricity, whereas a dominant t-phase results in antiferroelectricity. At an o-phase to t-phase ratio of 1:1, the sample displays MPB characteristics. Other peaks have minimal impact on the properties of HZO and are therefore omitted from the figure for clarity.

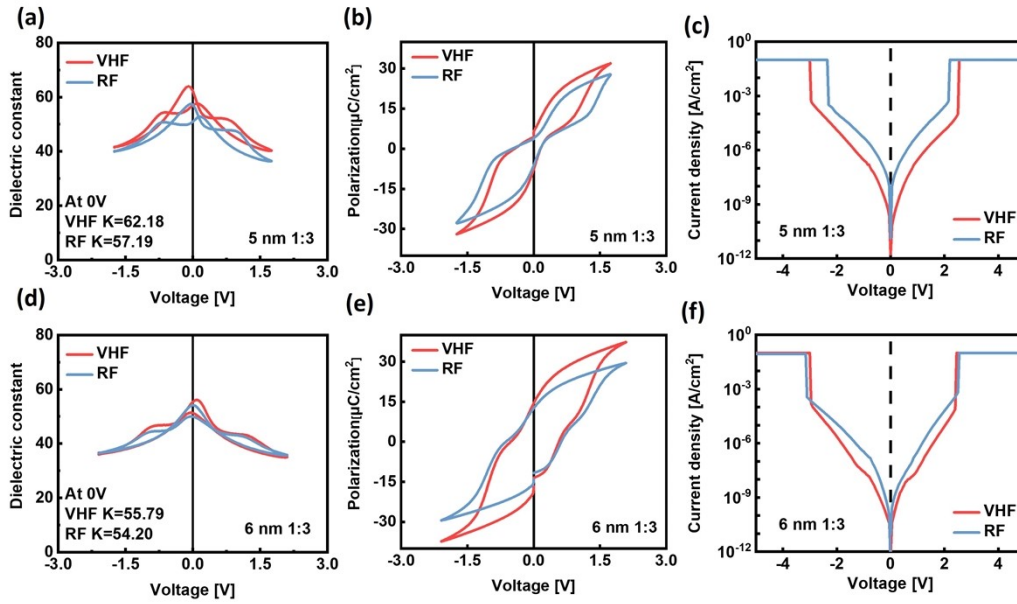


Figure S3. Basic characteristics of the 5 nm and 6 nm MPB HZO (1:3). The basic characteristics of the 5 nm MPB HZO (1:3) at room temperature are shown in (a) the Dielectric Constant-Voltage (D-V) curve, (b) the Polarization-Voltage (P-V) curve, and (c) the Current-Voltage (I-V) curve. Similarly, the basic characteristics of the 6 nm MPB HZO (1:3) at room temperature are presented in (d) D-V, (e) P-V, and (f) I-V.

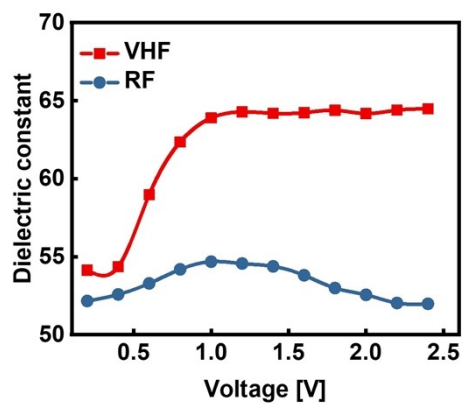


Figure S4. Dielectric constant of RF-deposited and VHF-deposited HZO films with voltage.

The VHF HZO film exhibits a non-flat curve, while the RF HZO film, which displays ferroelectric characteristics, shows a nearly flat curve resembling that of a dielectric capacitor. Moreover, the k value of the VHF HZO film increases in the low-field region, achieving an impressive k value of 63.89 even at 1 V.

PEALD Single Cycle Sequence

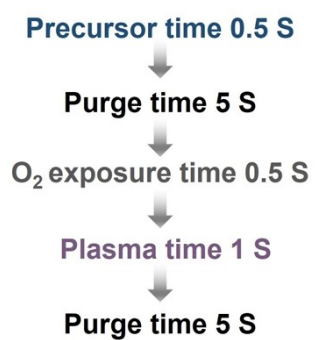


Figure S5. The steps involved in a single deposition.

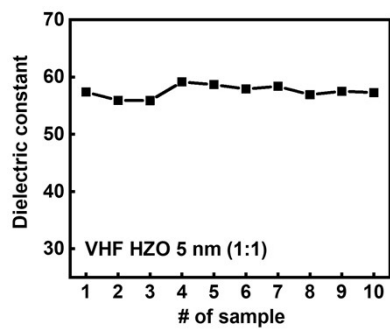


Figure S6. 10 different VHF HZO 5 nm (1:1) samples K value.

Dielectric Constant						
Thickness (nm)	VHF PE-ALD			RF PR-ALD		
	Hf:Zr ratio			Hf:Zr ratio		
	1:1	1:2	1:3	1:1	1:2	1:3
3	29.93	31.11	32.62	34.59	34.37	36.97
4.5	64.47	63.90	63.85	59.08	62.28	43.54
5	57.89	61.30	62.18	53.42	54.68	57.19
6	46.89	55.38	55.79	43.93	50.96	54.20
8	40.33	41.36	42.35	40.55	40.19	41.39

Table S1. Dielectric Constant of RF-deposited and VHF-deposited HZO films.

Table 1 compares the dielectric constants of HZO films deposited using VHF PE-ALD and RF PE-ALD, across film thicknesses ranging from 3 to 8 nm and Hf: Zr ratios of 1:1 to 1:3. The HZO films deposited with VHF PE-ALD exhibit higher dielectric constants.

Trap states (eV)	Thickness (nm)	Doping atom	Deposition method	Structure	Explanation	Ref.
1.36	16		ALD	TiN/HfO ₂ /TiN	Nitrogen containing defects	1
0.6 and 1.0	10		ALD	Pt/Ta ₂ O ₅ /HfO _{2-x} /TiN	Nanocrystalline grain boundaries	2
0.35-0.4	50		ALD	TiN/HfO ₂ /TiN	Oxygen vacancies	3
0.2	15		Sputtering	Al/ZrO ₂ /SiO ₂ /Si	Interstitial hydrogen atoms	4
0.3	4-6		Calculations	TiN/HfO ₂ /TiN	Interstitial hydrogen atoms	5
0.1	4-6		Calculations	TiN/ZrO ₂ /TiN	Interstitial hydrogen atoms	5
0.15–0.19	10	Zr	ALD	TiN/HZO/TiN	Interstitial hydrogen atoms	6
0.48–0.58	10	Zr	PLD	Pt/HZO/La _{0.7} Sr _{0.3} MnO ₃	Oxygen vacancies	7
0.6	10	Zr	PE-ALD	W/Hf _{0.5} Zr _{0.5} O ₂ /W	Oxygen vacancies	8
0.65	10	Zr	ALD	TaN/HZO/TaN	Oxygen vacancies	9
0.56	8.5	Al	ALD	TiN/HAO/Si	Oxygen vacancies	10
0.58	4.5	Zr	VHF PE-ALD	TiN/HZO/TiN	Oxygen vacancies	This work
0.42	4.5	Zr	RF PE-ALD	TiN/HZO/TiN	Oxygen vacancies	This work

Table S2. Trap states energy level of our sample and other reported hafnia films.

By comparing trap states with the references, we can determine that the main defects in VHF and RF HZO are oxygen vacancies¹⁻¹⁰.

Material	Ratio	Plasma frequency	Thickness (nm)	Growth Rate (Å/Cycle)
HZO	1:1	Very high frequency 100 MHz	3	1.57
			4.5	1.48
			5	1.35
			6	1.53
			8	1.55
		Radio frequency 13.56 MHz	3	1.35
			4.5	1.27
			5	1.20
			6	1.22
			8	1.31

Table S3. Deposition rate of the HZO (1:1) films.

Supporting Information References

1. D. S. Jeong, H. B. Park and C. S. Hwang, *Applied Physics Letters*, 2005, **86**.
2. J. H. Yoon, S. J. Song, I. H. Yoo, J. Y. Seok, K. J. Yoon, D. E. Kwon, T. H. Park and C. S. Hwang, *Advanced Functional Materials*, 2014, **24**, 5086-5095.
3. M. Lukosius, C. Walczyk, M. Fraschke, D. Wolansky, H. Richter and C. Wenger, *Thin Solid Films*, 2010, **518**, 4380-4384.
4. P. V. Aleskandrova, V. K. Gueorguiev, T. E. Ivanov and J. B. Koprinarova, *The European Physical Journal B - Condensed Matter and Complex Systems*, 2006, **52**, 453-457.
5. P. Peacock and J. Robertson, *Applied Physics Letters*, 2003, **83**, 2025-2027.
6. M. Park, H. Kim, Y. Kim, T. Moon, K. Kim, Y. Lee, S. Hyun and C. Hwang, *Journal of Materials Chemistry C*, 2015, **3**, 6291-6300.
7. X. Cheng, C. Zhou, B. Lin, Z. Yang, S. Chen, K. H. Zhang and Z. Chen, *Applied Materials Today*, 2023, **32**, 101804.
8. A. Mallick, M. K. Lenox, T. E. Beechem, J. F. Ihlefeld and N. Shukla, *Applied Physics Letters*, 2023, **122**.
9. Y.-H. Yeh, W.-C. Chen, T.-C. Chang, Y.-F. Tan, C.-W. Wu, Y.-C. Zhang, Y.-H. Lee, C. C. Lin, H.-C. Huang and S. M. Sze, *Semiconductor Science and Technology*, 2023, **38**, 085004.
10. C.-C. Yeh, T. Ma, N. Ramaswamy, N. Rocklein, D. Gealy, T. Graettinger and K. Min, *Applied Physics Letters*, 2007, **91**.